

Is non-Gaussianity sufficient to produce long-range volatile correlations?

Radhakrishnan Nagarajan

Abstract:

Scaling analysis of the magnitude series (volatile series) has been proposed recently to identify possible nonlinear/multifractal signatures in the given data [1-3]. In this letter, correlations of volatile series generated from stationary first-order linear feedback process with Gaussian and non-Gaussian innovations are investigated. We show that long-range correlations in the volatile series can be an outcome of non-Gaussian innovations.

Keywords: Detrended fluctuation analysis, volatility analysis.

PACS: 054.5 +b

Author for Correspondence

Radhakrishnan Nagarajan
Center on Aging, UAMS
629 Jack Stephens Drive, Room: 3105
Little Rock, AR 72205, USA
Email: nagarajanradhakrish@uams.edu

1. Introduction

Detrended fluctuation analysis (DFA) [4] and its extensions [1-3, 5-6] have been used widely to determine the nature of correlations in synthetic and experimental data obtained from a wide-range of complex systems. Recently [1-3], analysis of the magnitude series of the given empirical sample have been used to gain further insight into the underlying dynamics. More importantly, long-range correlation in the magnitude series was found to be indicative of nonlinear and possibly multifractal signatures in the given data [1-3]. In this letter, we show that long-range correlations in the volatility series can arise even in *linear* feedback processes under certain constraints.

2. Methods

First-order linear feedback process represents the most elementary of the stochastic processes, and is given by the expression

The process parameter \mathbf{q} determines the strength of the correlations and \in_n represents identical and independently distributed (i.i.d) process (white noise) sampled from a given distribution, also known as *innovations*. Each sample x_n is a weighted sum (linear combination) of innovations \in_n . For this reason (1) is also known popularly as linearly correlated noise. It can be shown analytically that the above process (1) is stationary for $|\mathbf{q}| < 1$ with associated auto-correlation function $\mathbf{r}(k) = \mathbf{q}^k$ (see Appendix). In the present study, we discuss the scaling behavior of linear feedback process (1) with Gaussian as well as non-Gaussian innovations \in_n are sampled from five different distributions, namely:

NORM: zero-mean unit variance innovations \in_n , sampled from a Gaussian distributed

white noise (g) with probability density function $f(g) = \frac{1}{\sqrt{2\pi}} e^{-x^2/2}, x \in (-\infty, \infty)$.

SQNORM: zero-mean unit variance innovations \in_n , sampled from squared transform of a Gaussian distributed white noise, i.e. $g_1 = g^2$.

EXPNORM: zero-mean unit variance innovations \in_n , sampled from exponential transform of a Gaussian distributed white noise i.e. $g_2 = e^g$.

UNI: zero-mean unit variance innovations \in_n , sampled from uniformly distributed white noise (u) with probability density function $f(u) = 1/(b-a), u \in (a, b)$.

LOGUNI: zero-mean unit variance innovations \in_n , sampled from negative log transform of a uniformly distributed white noise i.e. $u_1 = -\log(u)$.

The above abbreviations shall be used in the subsequent sections. It can be shown analytically that second order moments are sufficient to completely describe first order linear feedback process with Gaussian innovations. However, this is not true in the case of non-Gaussian innovations where higher order statistics are required to sufficiently describe the process. Two popular statistics used in literature to reflect the deviation from Gaussianity are skewness (\mathbf{y}) and kurtosis (\mathbf{k}). The distributions (NORM, EXPNORM, SQNORM, UNI and LOGUNI) along with their skewness (\mathbf{y}) and kurtosis (\mathbf{k}) statistics are shown in Figs. 1(a-e) respectively. While NORM and UNI are symmetric distributions ($\mathbf{y} = 0$), SQNORM, EXPNORM and LOGUNI are asymmetric ($\mathbf{y} \neq 0$). Linear feedback process ($q = 0.95$) generated with the above innovations along with their skewness (\mathbf{y}) and kurtosis (\mathbf{k}) statistics is shown in Figs. 1(f-j) respectively. It should be noted that skewness ($\mathbf{y} = 0$) and kurtosis ($\mathbf{k} = 3$) for (1) with uniformly distributed innovations (UNI) is similar to those with Gaussian innovations (NORM), Fig. 1.

3. Results

In the following discussion, DFA with fourth order polynomial detrending [2, 5], i.e. DFA(4) is used in order to minimize the effects of possible local trends on the scaling exponent estimate. The volatile series of the given data was generated as absolute value of their increments [1, 2] i.e. $v_n = |x_n - x_{n-1}|$. Since the processes considered are stationary first order linear feedback process, the number of samples was fixed at ($N = 2^{16}$, after discarding the initial transients). We believe that ($N = 2^{16}$) points should be sufficient to capture the statistical properties of such a primitive stochastic process.

Classical power-spectral analysis is used widely to investigate possible correlations in stationary linear processes. Power-spectrum of a stationary process is related to its auto-correlation function by the Wiener-Khinchin theorem. As noted earlier (Appendix), the expression of the auto-correlation for the first-order linear feedback process x_n (1) is governed solely by the process parameter q and is immune to the distribution of the innovations ϵ_n . Thus it might not be surprising to note that first-order linear feedback processes ($q = 0.95$) with Gaussian (NORM) and non-Gaussian (EXPNORM, SQNORM) innovations revealed similar spectral signatures, Fig. 1a, also reflected in the scaling of their fluctuation function $F(s)$ with time scale (s). However, the spectral signatures of their volatility series exhibited significant discrepancies, Fig. 1b. More importantly, volatility series of first order linear feedback process ($q = 0.95$) with non-Gaussian innovations (EXPNORM and NORM) exhibited dominant low-frequency characteristic of long-range correlated noise, unlike their Gaussian (NORM) counterpart. Subsequently, DFA (4) was used to investigate the scaling of 100 independent realizations of volatility series ($q = 0.95$) with Gaussian (NORM) and non-Gaussian (EXPNORM, SQNORM) innovations, Fig. 3. It is important to note that the EXPNORM and SQNORM were generated as the corresponding memoryless (static) nonlinear transforms of NORM, Sec. 2. Alternately, scaling of the volatility

series with Gaussian innovations (NORM) was used as an internal control and compared to those with non-Gaussian innovations (EXPNORM, SQNORM). Volatility scaling of the 100 independent realizations with Gaussian and non-Gaussian innovations is shown Fig. 3. It can be observed that the uncertainty in the scaling between the 100 independent realizations, as reflected by the slope of $\log_2 F(s)$ versus $\log_2(s)$, Fig. 3, is maximum at time scales ($> 2^{10}$). No reliable estimation of the scaling exponent is possible in this *noisy regime*, Fig. 3. Therefore, the scaling exponents were estimated at points which lie in the range [2^6 to 2^{10}]. As a comment, it should be noted that this region was kept fixed across the Gaussian (NORM) and the non-Gaussian processes (SQNORM, EXPNORM). Therefore, any discrepancy in the scaling exponents between the processes in this regime is solely due to their dynamics. The distribution of the scaling exponents estimated across 100 independent realizations of the three processes is shown in Fig. 4. While the distribution of the scaling exponents corresponding to Gaussian innovations (NORM) exhibited uncorrelated behavior ($\alpha \sim 0.5$), those corresponding to non-Gaussian innovations (EXPNORM, SQNORM) showed a significant deviation ($\alpha \gg 0.5$) from their Gaussian counterpart, Fig. 4. Statistical testing using parametric ttest rejected the null that the scaling exponents of the volatility series across with Gaussian innovations (NORM) were not significantly different from those with non-Gaussian innovations (SQNORM, EXPNORM) at significance level (0.05). Therefore, from the above discussion it is clear that volatility series of linear feedback process ($q = 0.95$) with non-Gaussian innovations exhibits long-range volatile correlations ($\alpha \gg 0.5$) unlike their Gaussian counterpart ($\alpha \sim 0.5$).

Similar to the above analysis, we generated 100 independent volatility series from linear feedback process with parameters ($q = 0.95$ and $q = 0.65$) and innovations sampled from uniformly distributed white noise (UNI) and its nonlinear counterpart (LOGUNI), Sec. 2. As in the previous case, we discarded points in the noisy regime and choose only those in the time scale [2^6 to 2^{10}]

for reliable estimation of the scaling exponent. The scaling of the volatility series corresponding to UNI and LOGUNI for parameters ($q = 0.95$ and $q = 0.65$) is shown in Figs. 5 and 6 respectively. The distribution of the scaling exponents estimated from Figs. 5 and 6 is shown in Figs. 7 and 8 respectively. It can be observed that the distribution of the scaling exponents for volatility series with uniformly distributed innovations (UNI) is similar to those of uncorrelated noise ($\alpha \sim 0.5$) whereas that of its nonlinear counterpart (LOGUNI) is similar to that of long-range correlated noise ($\alpha >> 0.5$) for parameters ($q = 0.95$ and $q = 0.65$), Figs. 7 and 8. Parametric ttest failed to reject the null that the distribution of the scaling exponents of the volatility series corresponding to non-Gaussian innovations UNI, Figs. 5 and 7 were significantly different from those obtained with Gaussian innovations ($\alpha \sim 0.5$), Figs. 3 and 4 at significance level (0.05). Statistical testing using ttest also revealed that the distribution of the scaling exponents for the volatility series corresponding to non-Gaussian innovations LOGUNI, Figs. 5 and 7, were significantly different from those of Gaussian innovations, Figs. 3 and 4. Varying the process parameter (q) also revealed that the overlap between distributions corresponding to UNI and LOGUNI increased with decreasing q .

Therefore, from the above results it is clear that linear feedback process with non-Gaussian innovations can give rise to long-range volatile correlations. It is also important to note that not all of non-Gaussian innovations give rise to volatile correlations. For the linear feedback process (1), the scaling exponent of the volatility series is governed by the process parameter q .

3. Discussion

Previous reports have shown that long-range volatile correlations may be an indicator of nonlinearity in the given data. However, in the present study we have shown that non-Gaussianity that manifest as innovations in linear feedback process may be sufficient to produce long-range

volatile correlations. Dynamical noise is an inherent feature of many complex systems and can be non-Gaussian in nature. Thus the present study also encourages a more detailed investigation of experimental data sets obtained from complex systems prior to inferring the nature of correlations in it.

Acknowledgements

I would like to thank the reviewers for helpful comments and suggestions. The present study is supported by funds from National Library of Medicine (1R03LM008853-1) and junior faculty grant from American Federation for Aging Research (AFAR).

Reference

1. Y. Ashkenazy, P.Ch. Ivanov, S. Havlin, C.-K. Peng, A.L. Goldberger and H.E. Stanley. Phys. Rev. Lett. 86 (2001), 1900.
2. Y. Ashkenazy, S. Havlin, P. Ch. Ivanov, C-K. Peng, V. Schulte-Frohlinde and H. E. Stanley. Physica A. 323 (2003), 19.
3. T. Kalisky, Y. Ashkenazy, and S. Havlin. Phys. Rev. E 72 (2005), 011913.
4. C.-K. Peng, S.V. Buldyrev, A.L. Goldberger, S. Havlin, F. Sciortino, M. Simons and H.E. Stanley. Nature 356 (1992), 168.
5. J.W. Kantelhardt, E. Koscielny-Bunde, H. A. Rego, S. Havlin, and A. Bunde. Physica A 295 (2001), 441.
6. J.W. Kantelhardt, S. A. Zschiegner, E. Koscielny-Bunde, S. Havlin, A. Bunde, and H. E. Stanley. Physica A 316 (2002), 87.

Appendix

Consider the first-order linear feedback process $x_n = \mathbf{q} x_{n-1} + \epsilon_n$, where ϵ_n are i.i.d innovations sampled from a white noise with a given distribution. The correlation between samples x_n and x_{n-k} is given by the expression

$$R(k) = E(x_n x_{n-k}), \text{ where } E \text{ represents the expectation operator}$$

For $k = 1$, we have

$$\begin{aligned} R(1) &= E(x_n x_{n-1}) = E((\mathbf{q} x_{n-1} + \epsilon_n) x_{n-1}) \\ &= \mathbf{q} E(x_{n-1} x_{n-1}) = \mathbf{q} R(0) \text{ as } E(x_{n-i} \epsilon_n) = 0 \text{ for } i > 0 \end{aligned}$$

Similarly, for $k = 2$, we have

$$R(2) = E(x_n x_{n-2}) = E((\mathbf{q} x_{n-1} + \epsilon_n) x_{n-2}) = \mathbf{q} E(x_{n-1} x_{n-2}) = \mathbf{q} R(1) = \mathbf{q}^2 R(0)$$

For the m^{th} lag, we have

$$R(m) = \mathbf{q}^m R(0)$$

The corresponding auto-correlation function is given by

$$\mathbf{r}(m) = \frac{R(m)}{R(0)} = \mathbf{q}^m \text{ which is stationary for } |\mathbf{q}| < 1.$$

It is important to note that the expression for the auto-correlation function $\mathbf{r}(m) = \mathbf{q}^m$ and the constraints on stationarity $|\mathbf{q}| < 1$ are immune to the distribution of ϵ_n .

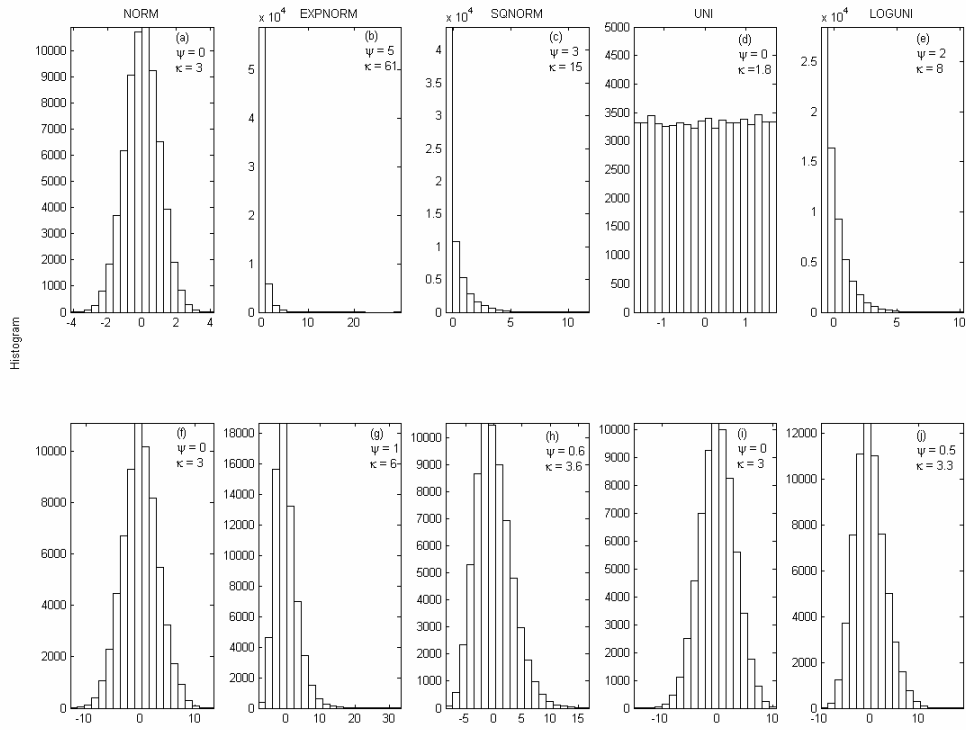


Figure 1 Histogram of Gaussian and non-Gaussian innovations namely: NORM, EXPNORM, SQNORM, UNI and LOGUNI along with their skewness (ψ) and kurtosis (κ) are shown in a-e respectively. Histogram of the first order linear feedback processes ($q = 0.95$) generated with the above innovations is shown right below them in f-j respectively.

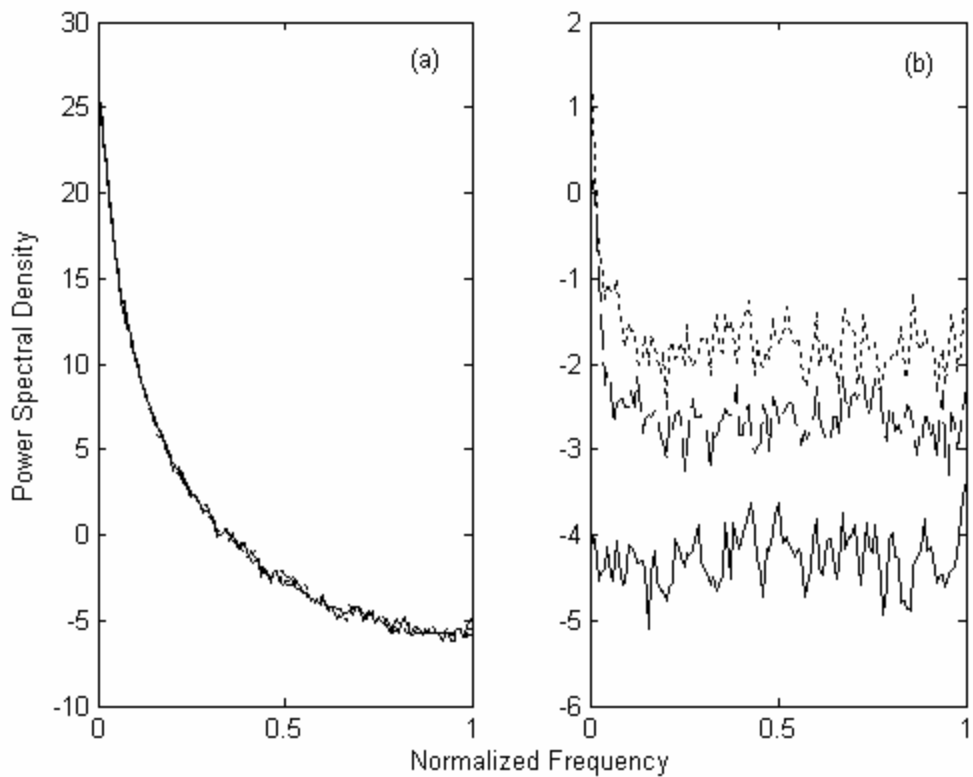


Figure 2 Power-spectral density ($\log S(f)$ versus f) for the first linear feedback ($q = 0.95$) with Gaussian (NORM) and non-Gaussian innovations (SQNORM and EXPNORM) (a) along with those of their volatility series (b).

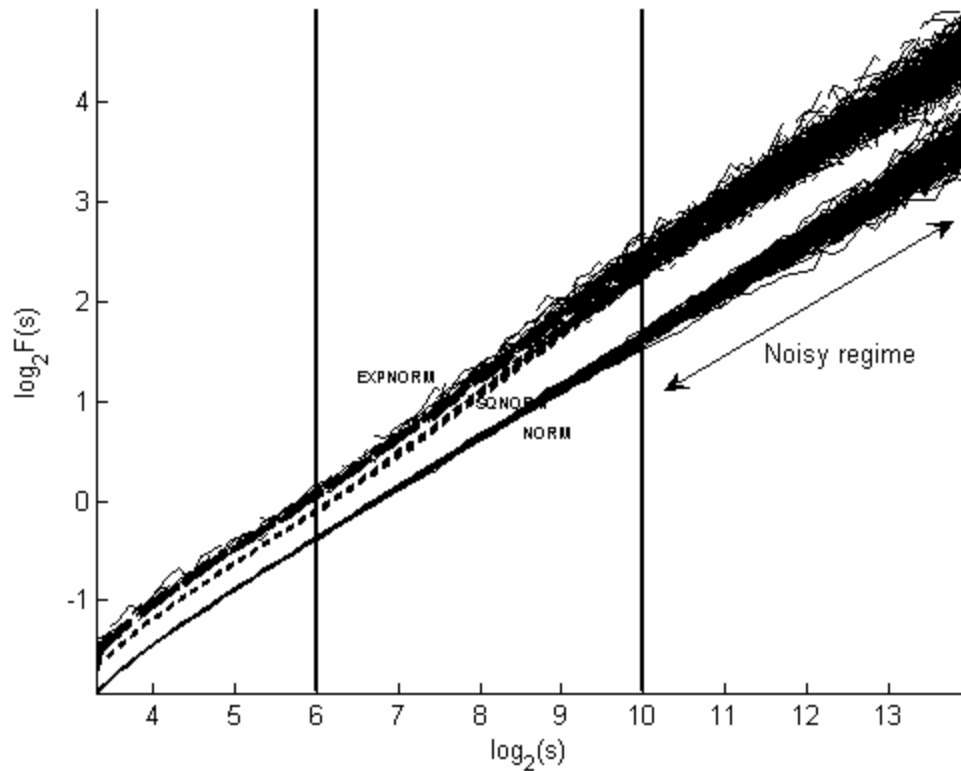


Figure 3 Plot of the fluctuation function $\log_2 F(s)$ versus time scale $\log_2(s)$ for 100 independent volatility series generated by the linear feedback process ($q = 0.95$) with Gaussian (NORM) and non-Gaussian innovations (SQNORM and EXPNORM), from bottom to top in that order. The vertical solid lines determine the region where the scaling exponents were estimated. The double-headed arrow represents the noisy regime.

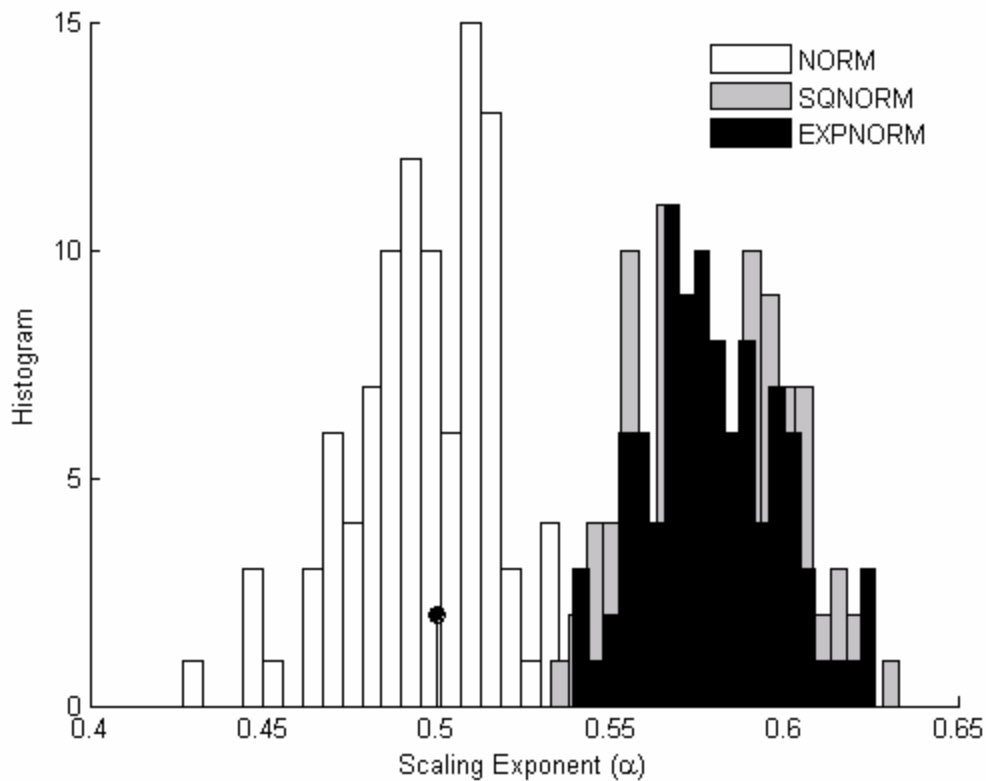


Figure 4 Histogram of the scaling exponent (α) estimates of the 100 independent volatility series, Fig. 3, generated by the linear feedback process ($q = 0.95$) with Gaussian (NORM) and non-Gaussian innovations (SQNORM and EXPNORM). Scaling exponent ($\alpha = 0.5$) corresponding to uncorrelated noise is shown as a reference (dark circle).

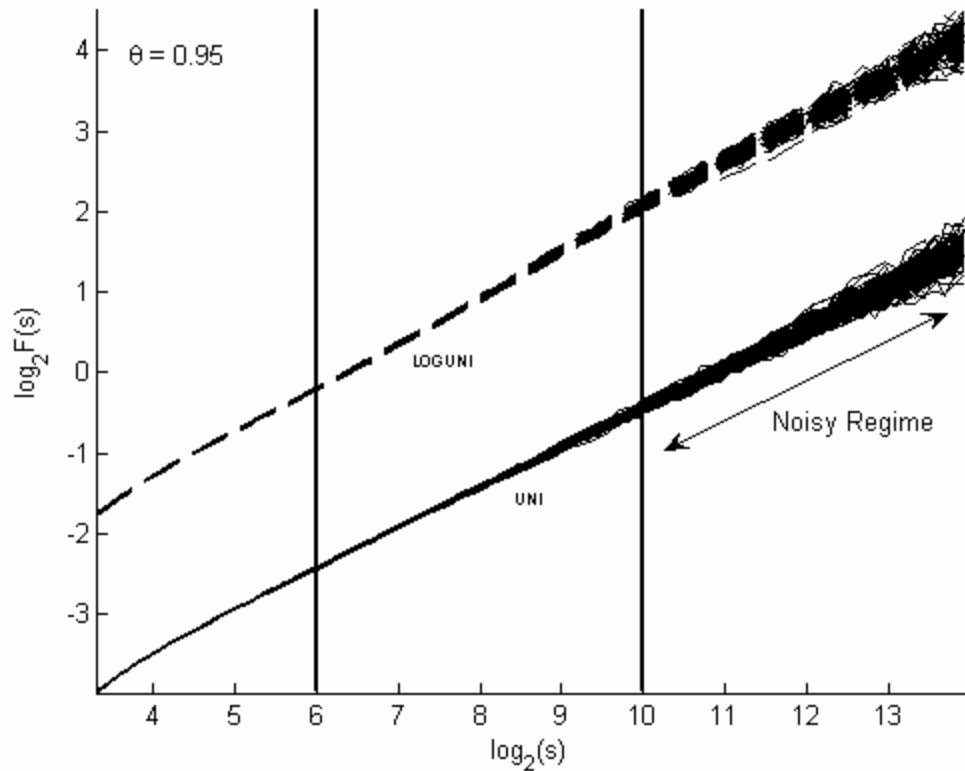


Figure 5 Plot of the fluctuation function $\log_2 F(s)$ versus time scale $\log_2(s)$ of 100 independent volatility series generated by the linear feedback process ($q = 0.95$) with uniformly distributed innovations (UNI) and its nonlinearly transformed counterpart (LOGUNI), from bottom to top in that order. The vertical solid lines determine the region where the scaling exponents were estimated. The double-headed arrow represents the noisy regime.

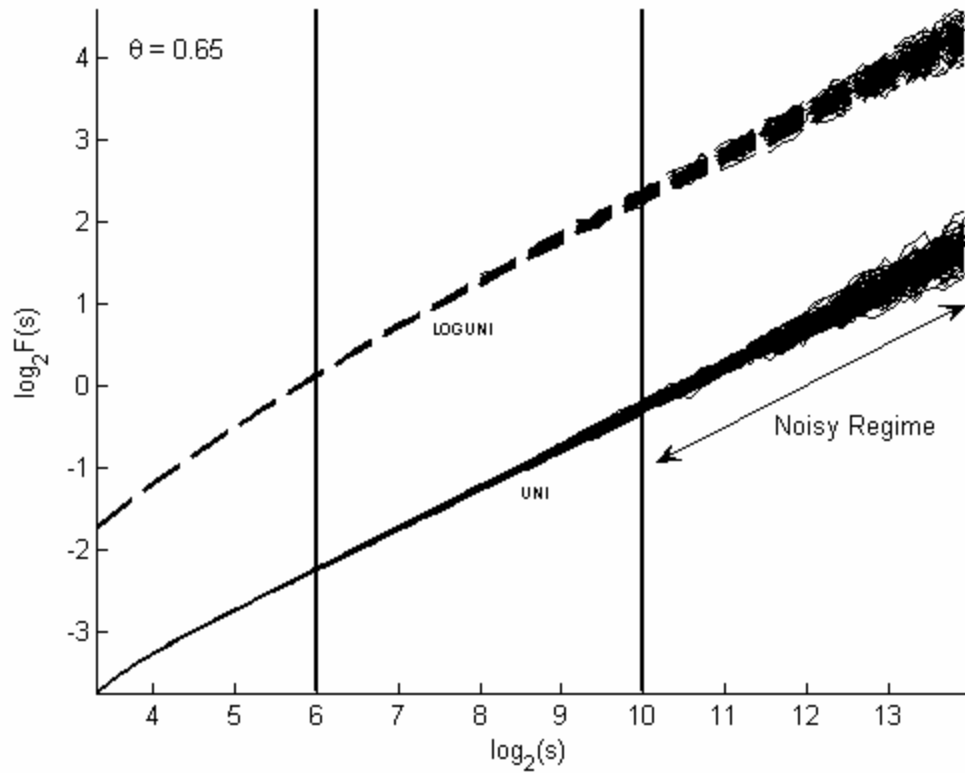


Figure 6 Plot of the fluctuation function $\log_2 F(s)$ versus time scale $\log_2(s)$ of 100 independent volatility series generated by the linear feedback process ($q = 0.65$) with uniformly distributed innovations (UNI) and its nonlinearly transformed counterpart (LOGUNI), from bottom to top in that order. The vertical solid lines determine the region where the scaling exponents were estimated. The double-headed arrow represents the noisy regime.

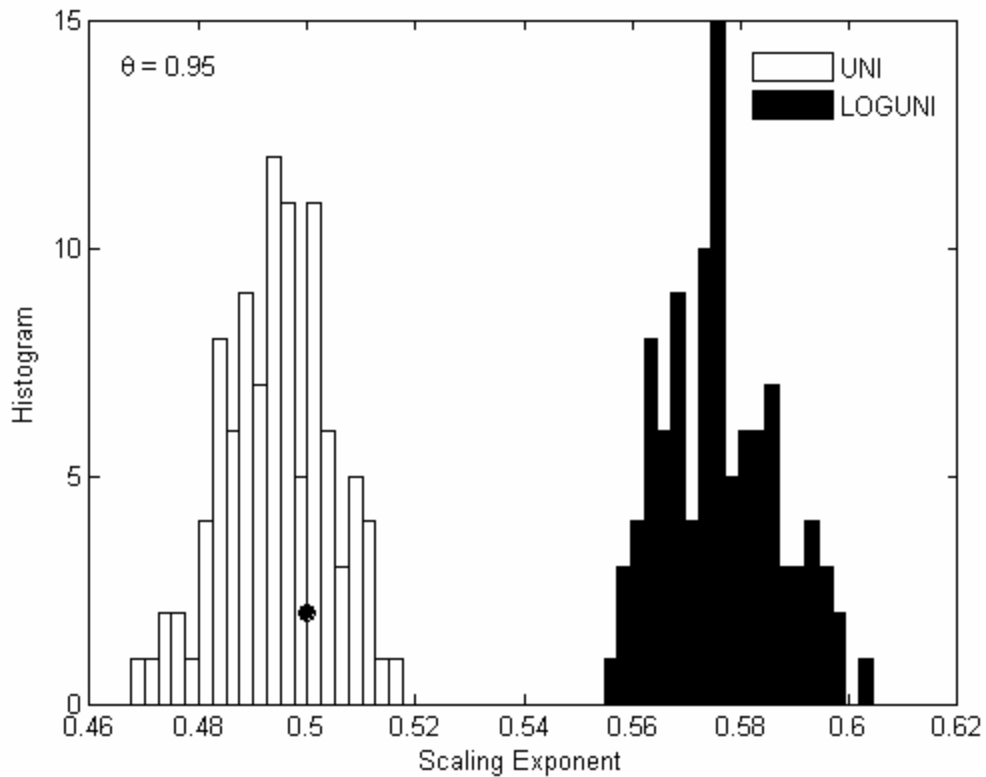


Figure 7 Histogram of the scaling exponent (α) estimates of 100 independent volatility series, Fig. 5 generated by linear feedback process ($q = 0.95$) with uniformly distributed innovations (NORM) and their nonlinear transformed counterpart (LOGUNI). Scaling exponent ($\alpha = 0.5$) corresponding to uncorrelated noise is shown as a reference (dark circle).

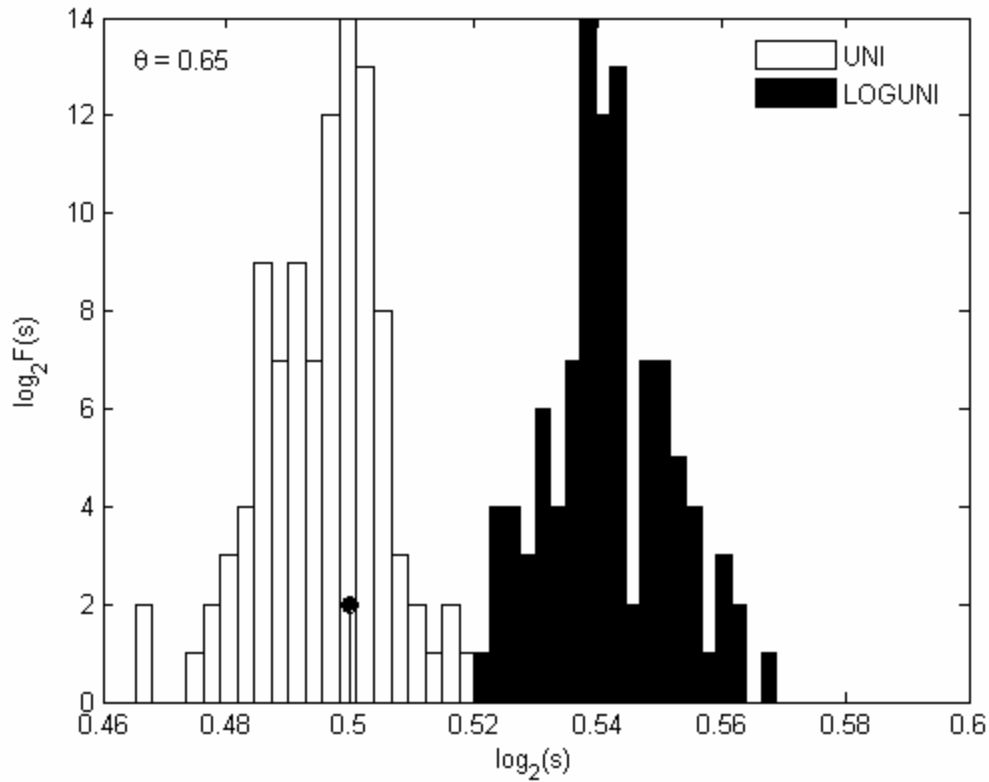


Figure 8 Histogram of the scaling exponent (α) estimates of 100 independent volatility series, Fig. 6, generated by linear feedback process ($q = 0.65$) with uniformly distributed innovations (UNI) and their nonlinear transformed counterpart (LOGUNI). Scaling exponent ($\alpha = 0.5$) corresponding to uncorrelated noise is shown as a reference (dark circle).